Heme Speciation in Alkaline Ferric FixL and Possible Tyrosine Involvement in the Signal Transduction Pathway for Regulation of Nitrogen Fixation†

Gudrun S. Lukat-Rodgers, Joey L. Rexine, and Kenton R. Rodgers*

Department of Chemistry, North Dakota State University, Fargo, North Dakota 58105-5516

Received June 17, 1998; Revised Manuscript Received August 3, 1998

ABSTRACT: The pH-dependent behavior of the ferric forms of two soluble truncations of *Rhizobium meliloti* FixL, FixL* (heme and kinase domains, functional), and FixLN (heme domain) are examined by UV−visible, resonance Raman, and electron paramagnetic resonance spectroscopy. Global analysis of UV−visible data indicates that the pK_a for hydroxide binding is slightly higher in FixL* than in FixLN. Spectroscopic data show that high-spin and low-spin hydroxide adducts of FixLN and FixL* exist in a thermal spin-state equilibrium with a significant fraction of the heme in the high spin form at room temperature. FixLN and FixL* differ from myoglobin and hemoglobin in that their hemes are not fully ligated by hydroxide ion under strongly alkaline conditions. In addition to the binding of hydroxide ion, both FixLN and FixL* undergo additional alkaline transitions that involve the deprotonation of tyrosine residues. FixLN contains four tyrosine residues. One has a pK_a of 9.6, which is indistinguishable from that for hydroxide binding to the heme. The other three tyrosines have pK_as greater than 11. At pH 11, the alkaline species react with cyanide to yield the familiar low-spin cyanide adduct. Upon reduction of the heme iron, the alkaline forms of the FixL deletion derivatives are converted to their deoxy forms. Resonance Raman spectra reveal that the Fe−His stretching vibrations of deoxyFixLN and deoxyFixL* are not measurably shifted from those of their neutral counterparts. Treatment of the alkaline deoxyFixLs with O_2 yields the respective oxy forms. Spectroscopic evidence indicates that the loss of activity at elevated pH cannot be attributed solely to generation of a low-spin heme hydroxide. Involvement of one or more tyrosines in signal transmission between the heme and kinase domains of FixL is proposed.

Heme proteins perform a broad range of functions including oxygen transport and storage, electron transfer, and catalytic disproportionation and reduction of the toxic oxidants superoxide and peroxide. Recently, a new class of heme proteins known as the heme-based sensors has emerged. It includes the NO sensor soluble guanylate cyclase (sGC[1]), the CO sensor CooA, and the O_2 sensor FixL. Their function is to sense the presence of small molecules that can act as heme ligands (*1*−*4*). Changes in ligand concentration modulate the populations of protein sensor molecules in the ligated and unligated states. These ligation states are accompanied by heme spin-state changes and, in the case of the NO sensor sGC, changes in coordination number that serve as a switch to generate the appropriate cellular responses. *Rhizobium meliloti* FixL is a key component of the signal transduction system that regulates expression of the nitrogen fixation genes *nifA* and *fixK* (*5*).

Rhizobium meliloti FixL contains a transmembrane domain, a heme-binding domain, and a kinase domain (*6*, *7*). The heme domain is a sensor domain that monitors oxygen concentration and regulates the autophosphorylation activity of its kinase domain in inverse proportion to $P(O_2)$ (*8*). Under aerobic conditions, oxygen is bound to the heme (oxyFixL) and autophosphorylation of the FixL kinase domain is inhibited. During symbiosis, anaerobic conditions result in loss of the heme-bound oxygen. This deoxyFixL (ferrous heme without oxygen bound) has an active kinase domain. Autophosphorylation of the kinase domain with ATP yields FixL-phosphate. Subsequent phosphotransfer from FixL-phosphate to FixJ produces FixJ-phosphate, the active form of this transcriptional activator for *fixK* and *nifA* genes (*9*−*11*).

Hemes are able to bind numerous small molecules and anions. The effect of these molecules on the spin state of the heme iron in FixL has been correlated with its kinase activity (*12*, *13*). Ligands that generate six-coordinate (6-c) low-spin (LS) complexes (O_2, CO, CN^-, imidazole) result in decreased kinase activity. High-spin (HS) complexes such as deoxyFixL, metFixL (ferric FixL), and metFixL-F exhibit kinase activity sufficient to generate FixL-phosphate.

The effects of pH on the structure, function, and coordination chemistry of heme proteins have been useful in elucidating important structural properties of their active sites. In alkaline solution, myoglobin (Mb) and hemoglobin (Hb) hydroxide complexes exist in thermal spin-state equilibria

† This research was supported by the U.S. Department of Agriculture (Award 96-35305-3628) and the Herman Frasch Foundation (Award 446-HF97).

* To whom correspondence should be submitted. Phone: 701-231-8746. Fax: 701-231-8831.

[1] Abbreviations: FixLN, heme domain of *Rhizobium meliloti* FixL; FixL*, heme and kinase domains of *Rhizobium meliloti* FixL; Mb, myoglobin; Hb, hemoglobin; HRP, horseradish peroxidase; heme−HO, heme heme-oxygenase; CIP, *Coprinius cinereus* peroxidase; CCP, cytochrome *c* peroxidase; sGC, soluble guanylate cyclase; rR, resonance Raman; EPR, electron paramagnetic resonance; CAPS, 3-[cyclohexylamino]-1-propanesulfonic acid; PIPES, 1,4-piperazinebis(ethanesulfonic acid); LS, low-spin; HS, high-spin; 6-c, six-coordinate; 5-c, five-coordinate.

S0006-2960(98)01439-1 CCC: $15.00
Published on Web 09/09/1998

(*14*−*19*). In contrast, alkaline forms of horseradish peroxidase (HRP), *Coprinus cinereus* peroxidase (CIP), and heme heme-oxygenase (heme-HO) exist primarily as LS hydroxide complexes (*20*−*24*). Examination of the alkaline forms of HRP, CIP, cytochrome *c* peroxidase (CCP), and several of their heme pocket mutants has established modes of distal H-bonding that can stabilize ligand complexes and H-bonding networks, which link their distal and proximal heme pockets (*24*−*26*).

In this study, the pH dependences of two *Rhizobium meliloti* FixL derivatives, FixL* and FixLN, are examined to ascertain how the spin state and ligation state of the heme in these sensor proteins respond to changes in pH. The soluble truncation of *Rhizobium meliloti* FixL, FixL*, contains the heme domain and the C-terminal kinase domain; it is capable of oxygen-binding, autophosphorylation (kinase activity), and phosphotransfer to FixJ (*6*). The protein FixLN, which contains only the heme domain, retains the ability to bind oxygen but lacks kinase activity (*7*). The pH dependence of heme ligation and spin-state distribution in FixLN and FixL* as revealed by UV−visible, resonance Raman (rR), and electron paramagnetic resonance (EPR) spectroscopies are reported here. These methods allow tracking of heme and tyrosine side chain speciation with changing pH.

MATERIALS AND METHODS

FixL* and FixLN of *Rhizobium meliloti* were expressed and purified as previously described (*7*, *27*). Protein purity was assayed by SDS−PAGE and by determination of the purity index, R_z. The R_z (A_{397}/A_{280}) was 4.00 and 2.56 for FixLN and FixL*, respectively. All UV−visible spectra were taken on a scanning double spectrometer under microcomputer control. UV−visible titrations were carried out with 2−10 μM protein in Tris/HCl or glycine/NaOH buffers; 1−2 μL aliquots of 0.5 M NaOH were added to change the pH. Reversibility of the titration data was confirmed by back-titration with small aliquots of 1 M HCl or by dialysis of alkaline samples into 50 mM Tris/HCl, pH 8.0. Global analysis of UV−visible spectrophotometric pH titration data was carried out using the SPECFIT program. The data were fit to four protic species, the smallest number to yield acceptable fits to titration curves at all peak maxima.

Samples for rR and EPR experiments were prepared by exchanging FixL* or FixLN into one of the following buffers: 100 mM CAPS, pH 10.7; 100 mM sodium carbonate−bicarbonate, pH 10.8 or 11.4; 100 mM glycine/NaOH, pH range 10.0−11.8; 100 mM Tris/HCl, pH 8.8 or 9.4; 100 mM sodium phosphate, pH 7.8; 100 mM PIPES, pH 7.0. Typical samples were 50−150 μM in protein and were made anaerobic by equilibration with nitrogen prior to use. Spectral features were independent of protein concentration.

Resonance Raman spectra were acquired from samples contained in a spinning 5-mm NMR tube using the 135° backscattering geometry and *f*1 collection. Low-frequency spectra of the Fe(II) forms of FixL were recorded using a 0.8-m scanning triple monochromator (*f*8), 441.6-nm excitation from a He/Cd laser, and a single photon counting detection system. High-frequency spectra of ferric FixL samples were acquired using a multichannel spectrometer as previously described (*28*). Raman excitation was accomplished either with 413.1- or 406.7-nm light from a Kr ion laser. Laser power at the sample never exceeded 15 mW for the ferric samples and 25 mW for the ferrous samples. To avoid photoreduction of the heme and/or laser-induced damage to the protein, cylindrical lenses were used to achieve a line focus at the sample and the sample tube was spun at ~20 Hz. In the variable-temperature experiments, the spinning sample tube was suspended in a liquid N_2 boiloff stream. A heater placed before the sample in the boiloff stream controlled the temperature to ±1 °C. The temperature of the sample was monitored by a thermocouple whose thermal junction was placed as close a possible to the sample without touching it. Absorption spectra were obtained before and after the rR experiments to verify sample integrity. The areas of ν_3 bands for the hydroxide adducts were obtained by curve fitting to a series of Lorentzian/Gaussian (1:1) peaks using the Marquardt−Levinberg algorithm. This line-shape function was shown, empirically, to accurately model single spectrally isolated solvent bands in spectra obtained with this spectrometer.

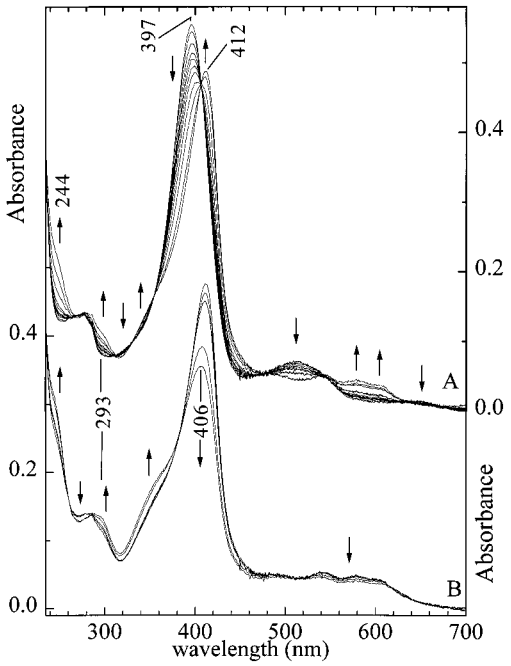

FIGURE 1: UV−visible spectrophotometric pH titrations for FixLN. (A) Group A pHs: 7.9, 8.4, 8.8, 9.0, 9.2, 9.4, 9.6, 9.9, 10.4, 10.9, and 11.0. (B) Group B pHs: 11.2, 11.5, 11.6, 11.8, and 11.9. ↑ indicates that as the pH increases, the absorbance of the feature also increases. ↓ indicates that as the pH increases, the absorbance at this wavelength decreases.

The EPR spectra were obtained at X-band on a spectrometer equipped with a 6 kG magnet and a liquid helium cryostat system. The EPR signals were referenced to solid pitch diluted in KCl. Spectra were acquired at 5 K with a microwave power of 0.2 mW, a 100 kHz modulation frequency, and a 10 G modulation amplitude. The reported spectra are summations of three scans.

RESULTS AND DISCUSSION

*pH Transitions in FixLN and FixL**. UV−visible spectra from the spectrophotometric pH titration of FixLN are shown in Figure 1. The general spectral features of ferric alkaline FixLN and ferric alkaline FixL* are similar. Two sets of isosbestic points are observed. The first set occurs in spectra

Table 1: Features of the Visible Spectra of Some Heme Hydroxide Proteins Complexes[a]

protein	pH	λ_{max}					spin state	ref
FixL*	10.7	410	[493]	543	579	604	LS/HS	this work
FixLN	11.0	412	[495]	543	579	604	LS/HS	this work
Mb[b]	10.5	412.5		539	585		LS/HS	*29*
Mb[c]	10.4	413	485	543	583	600	LS/HS	*19*
Hb	10.4	411	[~485]	541	576	600	LS/HS	*19*
HRP	12	415		543	575		LS	*19*
H42L HRP-C*[d]	12	411		546	575	602	LS/HS	*26*
H42R HRP-C*[d]	12	412		543	575	607	LS/HS	*26*
H52L CCP(MI)[e]	8.5	413.1		543	580		LS/HS	*25*
CIP[f]	12.1	412		543	575		LS	*24*
heme−HO	10.0	413		540	575		LS	*21, 30*

[a] Brackets indicate weak features. [b] Human Mb. [c] Sperm Whale Mb. [d] HRP-C*: recombinant horseradish peroxidase isoenzyme C. [e] C-CP(MI): cytochrome *c* peroxidase with extra N-terminal methionine and isoleucine. [f] CIP: *Coperinus cinereus* peroxidase.

of FixLN between pH 7.7 and 11.0 and for FixL* between 7.7 and 10.7. In these spectra, the Soret bands reach maximum extinction at 412 and 410 nm for FixLN and FixL*, respectively. These maxima are near those observed for hydroxide adducts of Mb and Hb (*19*, *29*) (Table 1). Thus, the visible spectra associated with the first set of isosbestic points indicate conversion of five-coordinate (5-c) ferric FixLN or FixL* to their corresponding 6-c hydroxide adducts. Presence of an additional alkaline form is indicated by the second set of isosbestic points observed above pH 11.0 for FixLN and above pH 10.7 for FixL*. Appearance of these isosbestic points is accompanied by a blue shift in λ_{max} for the Soret band. Formation of these alkaline species is reversible. The original pH 8.0 spectrum is obtained after alkaline FixLN or FixL* is dialyzed against pH 8.0 buffer. Also, back-titration of alkaline FixLN or FixL* with small aliquots of dilute HCl yields the same isosbestic points and titration curves as the titration with base.

Three tyrosine residues (Y190, Y197, and Y201) (*5*) flank the proximal histidine (H194) (*31*) in the primary sequences of both FixLs, indicating that the presence of tyrosine side chains in or close to the heme pocket is likely. Since FixLN contains four tyrosines and no tryptophans (*5*, *7*), the UV absorbance changes shown in Figure 1 can be evaluated in terms of tyrosine residues only. Tyrosine side chains exhibit absorbance maxima near 222 and 275 nm (*32*, *33*); tyrosinate has absorbance maxima near 240 and 293 nm (*33*). As the pH of FixLN is increased, absorbance features grow in at 293 and 244 nm. These spectral changes are consistent with deprotonation of tyrosine residues in the pH range where hydroxide complexes with the heme iron. Similar spectra are obtained for FixL*, which contains three additional tyrosine residues located in its kinase domain (*5*, *7*).

Figure 2 shows the Scatchard plot for formation of tyrosinate with increasing pH. The mole fraction of tyrosinates formed is determined from the change in the absorbance at 244 nm assuming $\epsilon_{244} = 11\,000\ M^{-1}\ cm^{-1}$ (*33*) for the tyrosinates in their FixL environments. These data show that FixLN has one tyrosine with a pK_a of 9.6 and three tyrosines with pK_as above 11.

The spectra in Figure 1 and those for the corresponding FixL* titration were analyzed by global least-squares analysis. The simplest model to produce an accurate fit to the data required four protic species. Figure 3 shows the fits

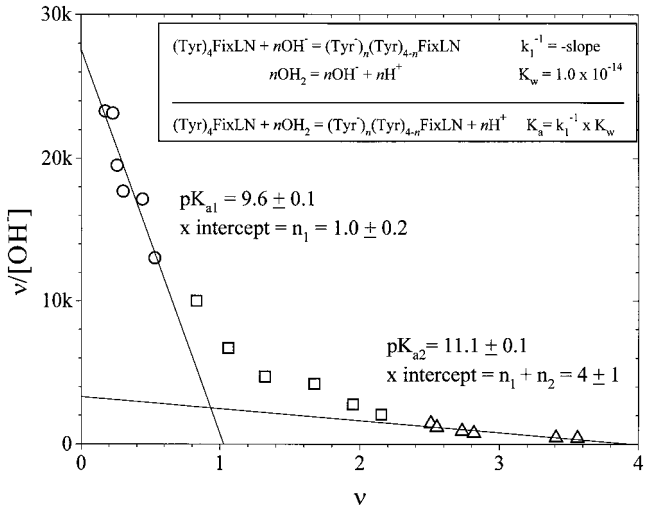

FIGURE 2: Scatchard plot for the generation of tyrosinate in FixLN. ○ points were used to determine k_1, pK_{a1}, and n_1. △ points were used to determine k_2, pK_{a2}, and $(n_1 + n_2)$. Equations in the inset show the relationship between k_i and pK_{ai}.

generated by this model for titration curves at wavelengths that monitor the disappearance of the 5-c neutral heme (397 nm) and the growth of the 6-c hydroxide adducts (410 and 604 nm). The pK_as obtained from the global fits are listed in Table 2.

The four-component spectra obtained from the global fit of the UV−visible titration data are shown in Figure 4. The spectrum of the neutral species (**1**) indicates that the heme is 5-c (*4*). The spectra of species **2** and **3** have similar absorbance features, indicating similarity in their hemes. The major difference between the spectra of **2** and **3** is the tyrosinate absorbance. The blue shift of the Soret band for species **4** suggests that it could be 5-c, which is confirmed by rR and EPR spectra discussed below. Changes in the heme and tyrosine absorption bands are summarized in the following equations:

$$(Tyr)_4FixLN\ [\mathbf{1}] + 2OH^- \rightleftharpoons (Tyr^-)(Tyr)_3FixLN{-}OH\ [\mathbf{2}] + H_2O \qquad K_{a1}$$

$$(Tyr^-)(Tyr)_3FixLN{-}OH\ [\mathbf{2}] + 3OH^- \rightleftharpoons (Tyr^-)_4FixLN{-}OH\ [\mathbf{3}] + 3H_2O \qquad K_{a2}$$

$$(Tyr^-)_4FixLN{-}OH\ [\mathbf{3}] + nOH^- \rightleftharpoons (Tyr^-)_4FixLN\ [\mathbf{4}] + nH_2O \qquad K_{a3}$$

The distributions of these four species as a function of pH were also extracted from the global fits and are shown for FixLN and FixL* in Figure 5, parts A and B, respectively. FixLN **2** grows in at lower pH and to a greater percentage than FixL* **2**. FixL* has three additional tyrosines, and the lower pK_{a2} observed for formation of FixL* **3** relative to FixLN **3** may be due to one or more of these additional tyrosines having a lower pK_a than those that deprotonate to form FixLN **3**. Since separate pH transitions cannot be identified for the individual tyrosine residues above pH 10.5, the apparent pK_{a2} reflects an average value. Although the distributions of **2** and **3** as a function of pH are different for

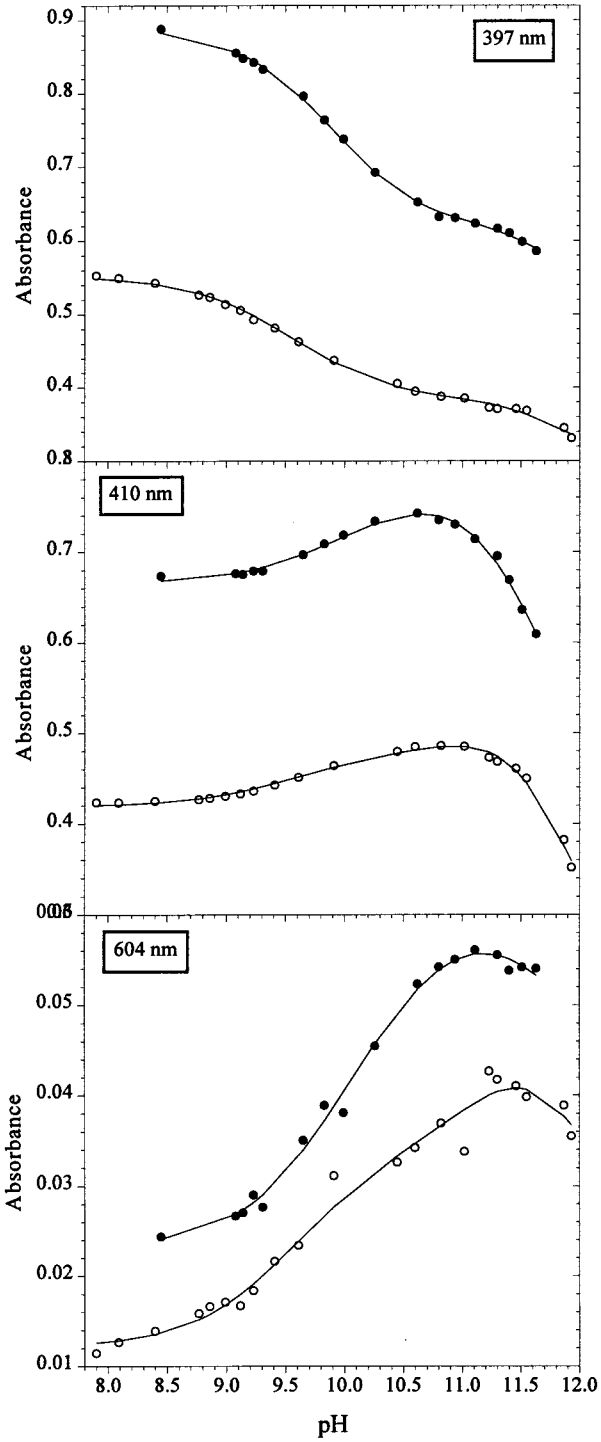

FIGURE 3: Titration curves for FixLN and FixL*. Solid lines represent the fits obtained from global least-squares analysis of titration data. Actual data points are indicated by ○ for FixLN and ● for FixL*.

Table 2: pK_as Determined from Global Fits

	FixLN	FixL*
pK_{a_1}	9.56 ± 0.03	9.93 ± 0.05
pK_{a_2}	11.43 ± 0.15	10.93 ± 0.14
pK_{a_3}	11.9 ± 0.1	11.75 ± 0.16

the two proteins, the maximum total fraction of heme with hydroxide bound is similar, with FixLN−OH and FixL*−OH reaching a maximum of 95% and 89%, respectively. This is shown by the sums of the curves for species **2** and **3** in

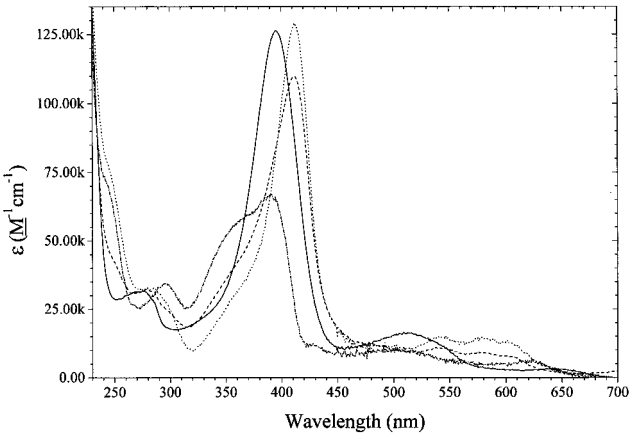

FIGURE 4: Spectra for the four species obtained from the global fit of the FixLN spectrophotometric titration: Solid line, neutral species (**1**); dashed line, $(Tyr^-)(Tyr)_3$FixLN−OH (**2**); dotted line, $(Tyr^-)_4$-FixLN−OH (**3**); dash−dot line, alkaline 5-c heme (**4**).

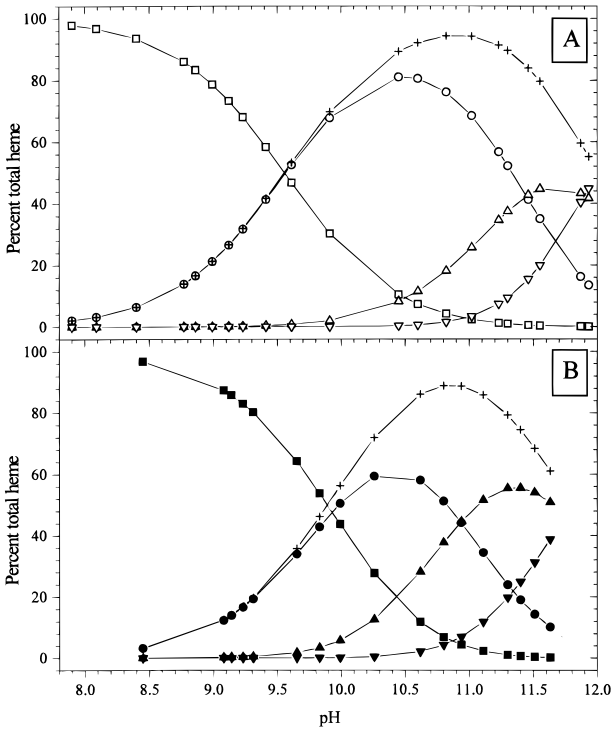

FIGURE 5: Distribution of species as a function of pH: (A) FixLN, open symbols and (B) FixL*, closed symbols. Data points for the four species for each protein are represented by the following symbols: ■, □, 5-c neutral heme protein; ●, ○, $(Tyr^-)(Tyr)_{n-1}$-FixL−OH; ▲, △, $(Tyr^-)_n$FixL−OH; ▼, ▽, 5-c alkaline heme protein; +, sum of $(Tyr^-)(Tyr)_{n-1}$FixL−OH and $(Tyr^-)_n$FixL−OH ($n = 4$ for FixLN).

Figure 5. Hence, the four-species model yields pK_as that characterize formation of FixLN−OH and FixL*−OH and which are similar to the previously reported value of 9.3, which was based on a single-wavelength determination (*4*).

Heme Spin-State Distribution in FixLN−OH and FixL−OH.* The features of visible spectra for ferric alkaline FixLN and FixL* are compared with those of other alkaline heme proteins in Table 1. The Q-band region of the spectra indicates that both HS and LS hydroxide forms of the FixL proteins are present in alkaline solution. By analogy to Mb−OH, the band at 604 nm is assigned to charge-transfer bands of the HS hydroxide-bound heme (*17, 34*). This band is absent from spectra of heme proteins that form only a LS

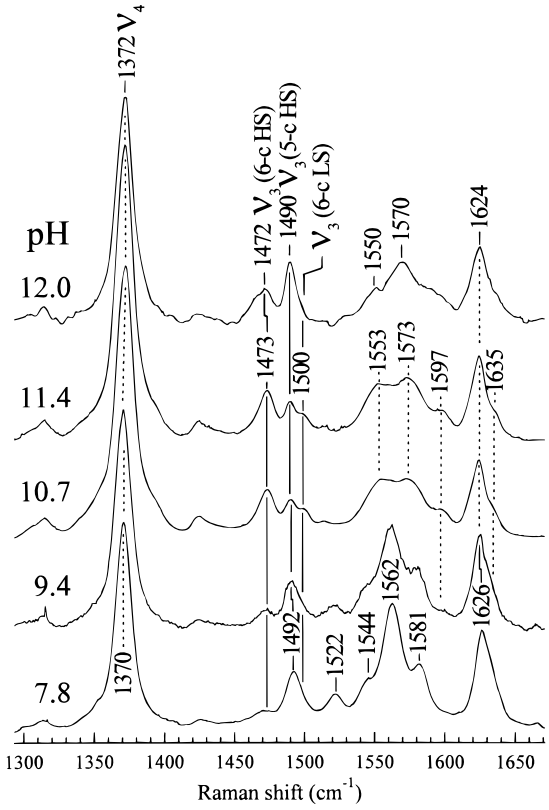

FIGURE 6: Resonance Raman spectra of ferric FixLN at indicated pH. Spectra were obtained at 20 °C with 413.1-nm excitation. Laser power was 15 mW at the sample.

hydroxide adduct (Table 1). The 543- and 579-nm bands are assigned to LS adducts by analogy with LS Mb−OH and Hb−OH (*19*). The relative intensities of the 604-nm band and the 579-nm bands are similar in spectra of alkaline FixLN and FixL*. The 604/579-nm intensity ratio is slightly lower than that observed for Mb−OH and higher than that reported for Hb−OH spectra at room temperature (*19*). These data indicate that the room-temperature HS/LS ratio for FixL−OHs lies between the 70:30 value for Mb−OH (*14*, *17*) and the 45:55 value for Hb−OH (*15*). Therefore, alkaline FixLs exist in thermal spin-state equilibria, with less than 55% of the hemes in the LS hydroxide form at room temperature.

It should be noted that spectra of species **2** and **3** both contain LS and HS absorbance features. The visible data (604/579-nm intensity ratio) indicate that these hydroxide adducts (**2** and **3**) are composed of HS and LS features that occur in a fixed ratio at a given temperature. Thus, the composite spectrum of the 6-c hydroxide adducts grows as that of a single species (*35*) and gives rise to the first set of isosbestic points. The second set of isosbestic points marks the interchange between the heme−hydroxides and species **4**. Hence, while all molecules of a given species (**2** or **3**) have the same elemental composition, they each comprise mixtures of HS and LS heme−hydroxide adducts.

Resonance Raman spectra of the alkaline FixLs are also indicative of this spin-state equilibrium. The pH dependence of the ferric FixLN Soret-excited rR spectrum is shown in Figure 6. Examination of ν_3 in these spectra is elucidating with respect to the spin state and coordination number of ferric alkaline FixLN. The ν_3 band, often referred to as the heme spin-state marker, falls in the characteristic frequency ranges for ferric hemes having the following permutations of spin state and coordination number: 1490−1500 cm^{-1} for HS 5-c, 1475−1485 cm^{-1} for HS 6-c, and 1500−1510 cm^{-1} for LS 6-c hemes (*36*, *37*). At pH 7.8, ν_3 occurs at 1492 cm^{-1}, indicating that ferric FixLN contains a HS 5-c heme iron (*27*). As the pH is raised, three species are evident based on three ν_3 bands at 1473, 1490, and 1500 cm^{-1}. These bands are assigned to HS 6-c FixLN−OH, HS 5-c FixLN, and LS 6-c FixLN−OH, respectively. The ν_3 frequencies for HS and LS 6-c FixLN−OH complexes are slightly lower than those observed for other ferric heme hydroxide complexes (see Table 3). At pH 12, the rR spectrum of FixLN is dominated by an alkaline 5-c HS species. The relative intensities of these bands were unchanged between 1 and 15 mW of laser power.

It is well established that low temperature favors the LS forms of Mb−OH and Hb−OH (*14*−*19*). Alkaline FixLN also shows this trend, as seen by the temperature dependence of its ν_3 intensities at pH 10.7 in Figure 7. As the temperature of FixLN is lowered, the 1473-cm^{-1} band decreases in intensity and, upon freezing, shifts to 1476 cm^{-1}. Upshifts of heme vibrations by a few wavenumbers are commonly observed upon freezing (*19*). Assignment of this band to the HS hydroxide adduct is confirmed by its loss of intensity at lower temperatures and the simultaneous decrease in intensity of the ν(Fe−OH) band for HS FixLN−OH at 479 cm^{-1} (*38*). As the 1473-cm^{-1} band disappears, the 1500-cm^{-1} band grows in intensity and shifts slightly to 1502 cm^{-1} upon freezing. At −100 °C, ν_{10} and ν(Fe−OH) of LS FixLN−OH are observed at 1638 and 542 cm^{-1} (*38*), respectively. Assignment of the 1638-cm^{-1} band as ν_{10} is based on (a) the similarity between its frequency and those reported for ν_{10} of other LS heme−hydroxide adducts (*17*, *19*, *30*, *40*, *41*) and (b) the fact that it is depolarized (*42*) in liquid solution (data not shown). The ν_3 band for HS 5-c FixLN persists at −100 °C.

The dependence of the metFixL* Soret-excited rR spectrum on pH is shown in Figure 8. Like FixLN, the heme is 5-c and HS in the pH 7.8 spectrum. At pH 10.7, the spectrum also contains three ν_3 bands, which correspond to HS and LS 6-c FixL*−OH and a HS 5-c species. At pH 11.4, bands from a HS 5-c alkaline species dominate the spectrum. The temperature dependence of these ν_3 band intensities is similar to that observed for ferric FixLN−OH. As the temperature is lowered, the LS ν_3 and ν_{10} intensities increase relative to those of HS FixL*−OH (data not shown), indicating that low temperature favors the LS FixL*−OH.

The relative amounts of HS and LS hydroxide complexes were examined by determination of the relative areas of the ν_3 bands at 1473 and 1500 cm^{-1}. Since it is not possible to isolate all components of this mixture of species, their Raman scattering cross sections could not be determined. Nevertheless, changes in the relative areas of these bands for a given protein would indicate shifts in species populations. Table 4 summarizes the relative areas of the ν_3 bands for FixLN−OH and FixL*−OH. Although these data do not allow quantitation of the HS and LS hydroxide species, they are consistent with a constant HS/LS ratio as the pH is raised. Within the detection limits of the rR experiment, species **2** and **3** have the same ratio of HS/LS hydroxide. Also, this HS/LS ratio is not significantly perturbed by the presence of the kinase domain if the relative resonance enhancements

Table 3: Resonance Raman Frequencies for Some Alkaline Heme Proteins[a]

protein	FixLN	FixL*	Hb	Mb	*Aplysia*Mb	H52LCCP	HRP	H42LHRP	heme−HO
pH	10.7	10.7	10.4	10.4	9.1	8.5	12.0	12.0	10.0
ν_3(6-c HS)	1473	1474	1478	1479	1478	1478	n.o.	1478	n.o.
ν_3(5-c HS)	1490	1490	n.o.	n.o.	n.o.	1492	n.o.	n.o.	n.o.
ν_3(6-c LS)	1500	1500	1503	1504	1506	1504	1504	1506	1503
ν_4	1372	1374	1375	1373	1374	n.r.	1378	1377	1376
ν_{10}(6-c HS)	*	*	1604	1607	n.r.	*	n.o.	n.r.	n.r.
ν_{10}(6-c LS)	1635	1634	1636	1640	n.r.	1637	1640	1640	1638
ν(Fe−OH)$_{HS}$	479	477	492	491	n.r.	n.r.	n.o.	493	n.o.
ν(Fe−OH)$_{LS}$	539	539	553	550	n.r.	n.r.	503	n.o.	546
ref	*b, 38*	*b, 38*	*17, 19*	*17, 19*	*39*	*25*	*19, 20, 40*	*26*	*21, 22, 30*

[a] *, unable to assign because of significant overlap with other bands; n.r., not reported; n.o., not observed. [b] This work.

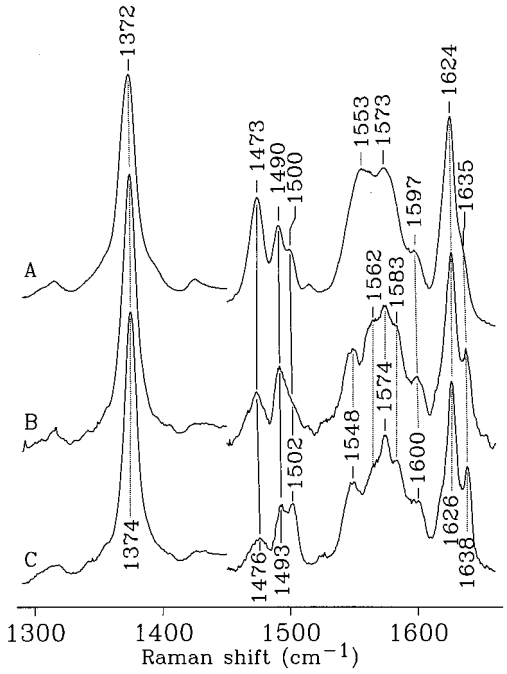

FIGURE 7: Resonance Raman spectra (413.1 nm excitation) of alkaline ferric FixLN as a function of temperature: (A) 20 °C, (B) −50 °C, and (C) −100 °C. The region from 1450 to 1660 cm^{-1} is expanded 2.8 times relative to the ν_4 band in each of the spectra. Laser power was 10 mW at the sample.

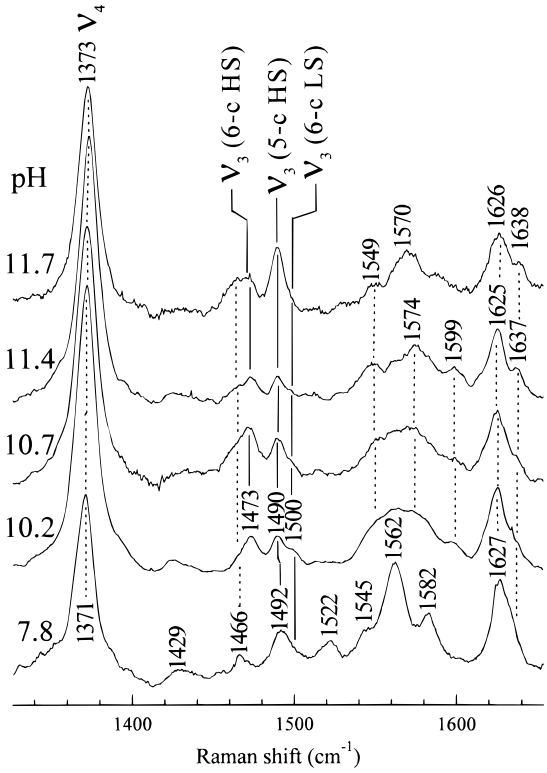

FIGURE 8: Resonance Raman spectra of ferric FixL* at indicated pH. The 413.1-nm excited spectra were obtained at 20 °C with 15 mW at the sample.

for these bands in FixLN−OH and FixL*−OH are assumed to be comparable. The 0.37 increase in pK_{a1} for FixL* might be expected to correlate with a small change in the HS/LS ratio for FixL*. If this occurs, the change in HS/LS is within the uncertainty of the ratio as determined from our rR spectra.

The speciation observed by visible and rR spectroscopies is also evident in the EPR spectra of FixLN and FixL*. Figure 9 shows the X-band EPR spectra for ferric FixLN between pH 7.0 and 12.0. At pH 7.0, metFixLN exhibits an EPR spectrum with signals at 6.16 (g_1), 5.75 (g_2), and 1.99 ($g_{||}$). The $g_\perp$ value [($g_1 + g_2$)/2] is 5.96, which indicates that the heme in FixLN is virtually all HS with $S = 5/2$ (*43*). At pH 7.0, ferric FixLN and FixL* exhibit rhombic HS EPR spectra similar to those observed for the distal His Mb mutants H64L, H64V, H64T, and H64I (*44*, *45*). These mutants have been shown to be pentacoordinate, in contrast to hexacoordinate native aquometMb, which exhibits an axial $S = 5/2$ EPR signal ($g = 5.95$, 1.99) (*44*−*46*). The EPR data reported here are consistent with visible data (*4*) and rR data (*27*) that suggest the neutral ferric FixL proteins are pentacoordinate. The percent rhombicity (R) for neutral

Table 4: Comparison of Areas of ν_3 for HS and LS Hydroxide Adducts of FixLN and FixL* in Spectra Obtained with 413.1 and 406.7 nm Excitation

		ratios of ν_3 areas for six-coordinate hydroxide adducts	
protein	pH	HS 6-c/total 6-c	LS 6-c/total 6-c
		413.1 nm Excitation	
FixLN	10.0	0.74	0.26
	10.7	0.75	0.25
	11.4	0.76	0.24
FixL*	10.7	0.74	0.26
		406.7 nm Excitation	
FixLN	10.7	0.74	0.26
	11.4	0.77	0.23
FixL*	10.2	0.74	0.26
	10.7	0.70	0.30

FixLN is 2.5 ($R = [\Delta g/16] \times 100$, where $\Delta g = |g_1 - g_2|$ (*46*)). As pH is increased, R of the HS signal increases ($R = 3.1$ at pH 11.0) and a feature grows in at $g = 6.04$. At pH 11.0 and 12.0, the HS EPR spectrum contains axial HS

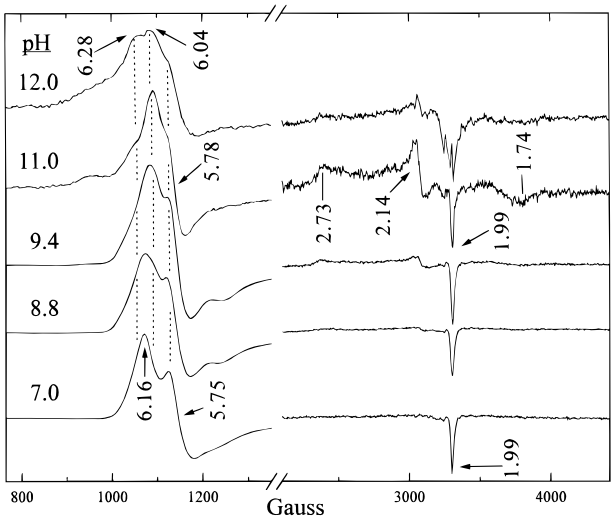

FIGURE 9: X-band electron paramagnetic resonance spectra for FixLN as a function of pH. All spectra were acquired at 5 K. The amplitudes of the high-field region have been multiplied by a scale factor of 4.

Table 5: Comparison of the Effective *g* Values of EPR Spectra of Ferric Low-Spin Heme Hydroxide Protein Adducts

protein	*g* values			reference
FixLN	2.73	2.14	1.74	this work
FixL*	2.73	2.14	1.74	this work
whale Mb	2.55	2.17	1.85	*47*
human Mb	2.59	2.16	1.84	*44*
human H64Q Mb	2.53	2.17	1.86	*44*
Aplysia Mb	2.67	2.15	1.77	*48*
legHb a	2.54	2.19	1.84	*49*
Lucina Hb I	2.66	2.17	1.82	*47*
Lucina Hb II	2.61	2.20	1.82	*47*
heme−HO	2.67	2.21	1.79	*21*

features from FixLN−OH superimposed on a rhombic HS 5-c FixLN spectrum.

In addition to changes in the HS EPR signatures, features indicative of a LS species appear in the EPR spectra of ferric FixLN as the pH is raised to 11.0 and decrease at pH > 11.0. The pH dependence of these features tracks that for growth of the LS ν_3 bands in the rR spectra (Figure 6). The *g* values for LS FixLN−OH and LS FixL*−OH are 2.73, 2.14, and 1.74. These LS FixL−OH adducts differ from other LS heme protein hydroxide complexes by their high g_z value as shown in Table 5. The rhombicity (V/Δ) and tetragonality (Δ/λ) parameters (*43*) determined from these *g* values are 0.51 and 5.8, respectively. The rhombicity is similar to that of Hb−OH (0.53). However, the tetragonality of the FixL−OHs is lower than that of Hb−OH (6.6). This is consistent with the low ν(Fe−His) (*27*, *50*) and ν(Fe−OH) (*38*) frequencies in deoxyFixLs and FixL−OHs, respectively, which reflect weaker bonds and a weaker axial ligand field than those in the corresponding Hb derivatives. It should be noted that although LS ferric heme signals are easily saturated at the low temperature used to obtain high-quality spectra of the HS heme, the microwave power was sufficiently low (0.2 mW) to not saturate the LS signal. This was demonstrated by measuring the low-spin amplitude as a function of microwave power (data not shown).

The presence of 5-c HS forms of FixLN and FixL* in alkaline solution distinguishes these proteins from Hb and

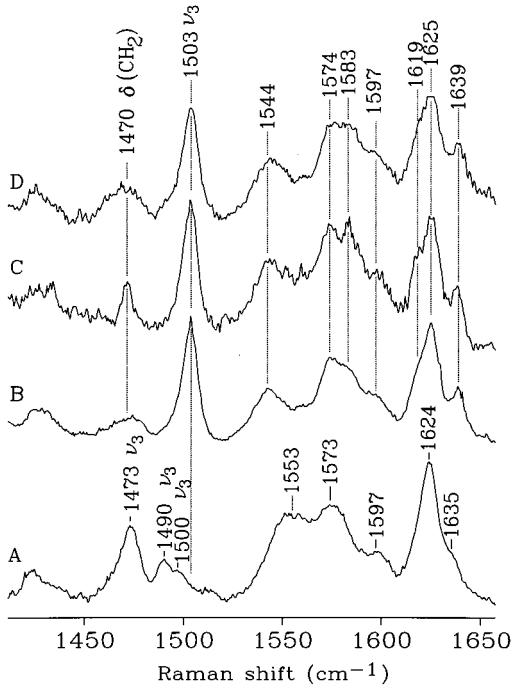

FIGURE 10: The 413.1-nm excited room-temperature resonance Raman spectra of (A) FixLN in 100 mM glycine, pH 11.0, (B) sample in (A) reacted with excess sodium cyanide, (C) FixLN in 50 mM Tris/HCl, pH 7.8, reacted with excess sodium cyanide, and (D) FixL* in 100 mM glycine/NaOH pH 11.0, reacted with excess sodium cyanide.

Mb, which are completely ligated by hydroxide ion at pH ≥ 10.4 (*19*). The ferric FixL proteins have a lower affinity for OH^- than the globins listed in Table 3. This reduced OH^- affinity is consistent with the lower ν(Fe−OH) frequencies (and therefore, weaker Fe−O bonds) for FixL proteins (*38*) compared to those for Hb and Mb (*17*, *19*). In addition to this intrinsically low affinity for hydroxide, a third high-pH alkaline transition lowers the affinity even further (*4*), perhaps due to partial denaturation of the protein. The affinity of FixL* for OH^- is more sensitive to the effects of increasing pH. The speciation diagrams in Figure 5 show that the hydroxide adducts of FixL* grow in and disappear over a narrower pH range than the corresponding species of FixLN. Although the structural basis for the decreased affinity in FixL* relative to FixLN is not clear, a general negative effect of the kinase domain on the heme's affinity for ligands has been observed (*4*, *13*, *27*).

*Binding of Strong-Field Ligands to Alkaline FixLN and FixL**. All forms of ferric alkaline FixLN and FixL* react with cyanide ion. The rR spectra in Figure 10 show that all three alkaline ferric FixLN ν_3 bands are replaced by a single ν_3 band upon formation of FixLN−CN at pH 11.0. The ν_3 band for both the low- and high-pH cyanide adducts occurs at 1503 cm^{-1}. The ν_2 (1583 cm^{-1}) and ν_{10} (1639 cm^{-1}) frequencies for alkaline FixLN−CN are also typical of LS 6-c ferric heme complexes (*37*). The same behavior is observed upon treatment of ferric FixL* with cyanide at pH 11.0 (Figure 10D).

Upon reduction with sodium dithionite, all forms of alkaline ferric FixL*, the HS 6-c hydroxide, the LS 6-c hydroxide, and the HS 5-c species, are converted to deoxy-FixL* as shown by the rR spectra in Figure 11. The high-frequency rR spectrum obtained for alkaline deoxyFixL* (ν_2,

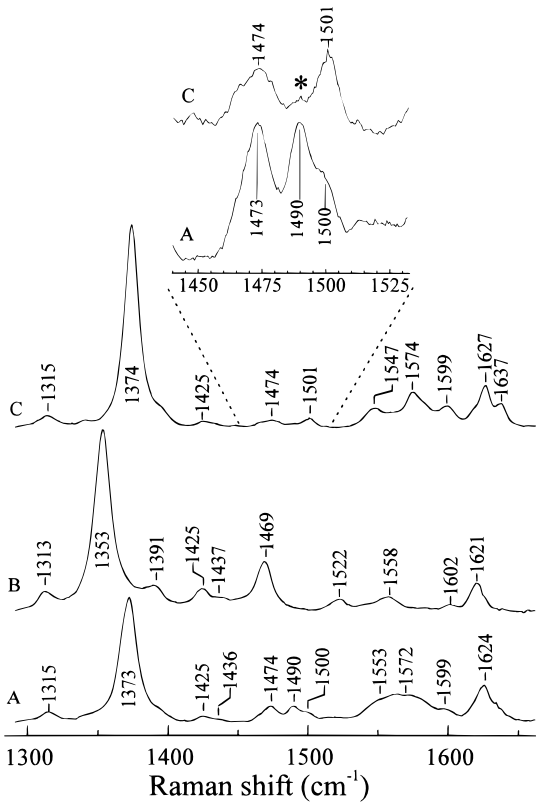

FIGURE 11: Conversion of alkaline FixL* to oxyFixL* as monitored by 413.1-nm excited resonance Raman spectroscopy: (A) FixL* in 100 mM glycine, pH 10.2; (B) sample in (A) reduced with 5-fold excess of sodium dithionite to generate deoxyFixL* at pH 10.2; (C) sample B flushed with O_2. Inset shows expansion of the ν_3 region of the spectra A (alkaline FixL*) and C (oxyFixL*, pH 10.2). The ν_3 for alkaline 5-c HS is indicated by *. With time under aerobic conditions, the heme auto-oxidized and the sample gave a spectrum identical to that shown in A. All of these spectra were obtained at 20 °C with 10 mW of laser power at the sample.

1558 cm^{-1}; ν_3, 1469 cm^{-1}; ν_4, 1353 cm^{-1}) is consistent with the previously reported pH 7.8 deoxyFixL* spectrum (*28, 50*). The addition of O_2 to the alkaline deoxyFixL* yields oxyFixL* with ν_2 (1574 cm^{-1}), ν_3 (1501 cm^{-1}), and ν_4 (1374 cm^{-1}) (Figure 11) in good agreement with those previously reported at pH 7.8 (*50*). Thus, all alkaline FixL* species present at pH 10.2 are converted to a single ferrous FixL* form, which binds O_2. Oxygen binding to FixLN at pH 12 and to FixL* at pH 11.6 was also corroborated by their UV−visible spectra. After a short time under an O_2 atmosphere, the hemes are auto-oxidized to their alkaline ferric forms, which has been observed for FixL proteins at pH 7.0 (*4*). These O_2 binding experiments show that the proteins are not completely unfolded or denatured under conditions where the high-pH 5-c HS alkaline species is present. If the heme pocket structure were completely disrupted, it is unlikely that O_2 binding would be observed.

Effect of Alkaline Transitions on Fe−His Bond Strength. The low-frequency 441.6-nm rR spectra of deoxyFixL* at pH 7.8 and 11.0 are shown in Figure 12. Small intensity changes are observed for bands at 381 and 284 cm^{-1}. The 381-cm^{-1} band is tentatively assigned to the $\delta(C_\beta C_c C_d)$ propionate bending modes by analogy to Mb, CCP, and HRP (*19, 51, 52*). The other band is currently unassigned. The ν(Fe−ImH) frequency (210.5 cm^{-1}) is unperturbed at the elevated pH, even though the tyrosines in the vicinity of the

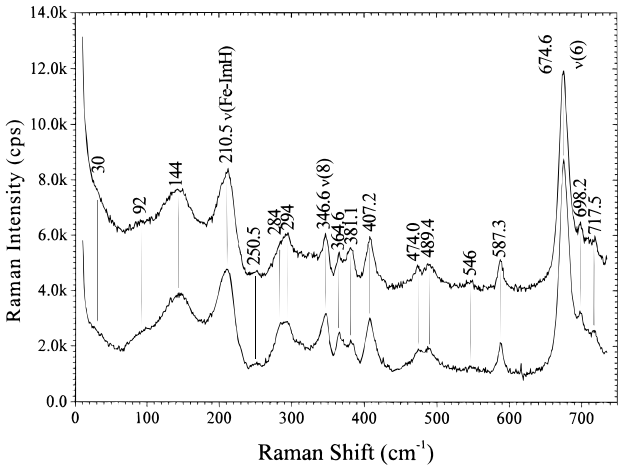

FIGURE 12: Low-frequency rR spectra of deoxyFixL* obtained with 441.6 nm excitation. Top: deoxyFixL* in 100 mM glycine, pH 11.0. Bottom: deoxyFixL* in 100 mM Tris/HCl, pH 7.8.

heme are deprotonated at pH 11.0 in both proteins. In CCP (*41, 52−54*) and HRP (*55*), where the proximal histidine has partial imidazolate character due to strong H-bond donation to aspartate side chains, ν(Fe−Im) is ∼30 cm^{-1} higher than that observed for FixLs. Thus, the protonation state/H-bonding status of the proximal imidazole in FixLN and FixL* is unchanged between pH 7.8 and 11.0.

Possible Role of Tyrosine in Signaling. The spin-state model for kinase inactivation argues that generation of a LS heme iron holds FixL in a conformation that precludes autophosphorylation (*12*). Low-spin FixL*−OH would be inactive while HS FixL*−OH would be active by analogy with LS FixL*−CN and HS FixL*−F, respectively. The 5-c alkaline form may not be active if it is indeed partially unfolded. The autophosphorylation activity of FixL between pH 8.5 and 11.0 is reported to decrease 5-fold with its midpoint at pH 9.5 (*12*). Hence, the loss of kinase activity tracks the first pH transition of FixLN and FixL* (Figures 3 and 5), which is shown herein to reflect OH^- coordination to the heme and deprotonation of a single tyrosine residue. To account for the observed loss of kinase activity, the spin-state model requires ∼80% of the heme to be in the LS form at pH 11 and room temperature. Since pH 11 solutions of FixLN and FixL* contain between 30 and 55% LS adducts, the loss of activity cannot be accounted for entirely by generation of LS hemes or unfolding. The speciation revealed by spectroscopic data presented here shows an interesting correlation between the simultaneous formation of heme−OH and a single heme domain tyrosinate and the midpoint of the pH dependence of kinase activity (*12*). This correlation, together with the heme−OH spin-state distribution, suggests that the HS hydroxide adduct is partially inactivated. This inactivation is unlikely to result from complete denaturation of the heme pocket, as the heme still binds O_2 to yield the oxyFixL* and the proximal Fe−ImH bond in the deoxy form is intact at pH 11. However, conformational changes are evident in the heme pocket. The increase in intensity of the $\delta(C_\beta C_c C_d)$ band in the high-pH spectrum of deoxyFixL* suggests changes in a heme propionate conformation. This is also supported by broadening of the propionate CH_2 deformation bands, $\delta(CH_2)$, in the pH 11 rR spectra of FixL−OHs (1466 cm^{-1}) and FixL−CNs (1470 cm^{-1}). Because of the possible proximity of a

tyrosine to the carboxylate group of one or both heme propionate substituents, the broadening of their $\delta(CH_2)$ bands could result from changes in their H-bonding status upon tyrosine deprotonation. We propose that tyrosine deprotonation between pH 8.5 and 11.0 may elicit conformational changes, which in turn, contribute to the observed decrease in kinase activity. This suggests that deprotonation of tyrosine residue(s) may destabilize one or more H-bond interactions required for transmission of the signal that regulates the kinase activity. Inactivation of the kinase could be explained in terms of changes in H-bonding that are not directly detectable by the spectroscopic probes used in this study. However, correlation between the midpoint of pH-dependent kinase inactivation and the pK_a for formation of heme−OH and tyrosinate implicates these two structural changes in the loss of activity.

SUMMARY

The spectroscopic data presented indicate that FixLN and FixL* go through three acid/base transitions as the pH is raised. First, the hemes are converted from ferric 5-c HS to a mixture of 6-c HS and LS hydroxide adducts in concert with deprotonation of one tyrosine side chain in the heme domain. The second transition involves deprotonation of additional tyrosines. The third transition results in formation of an alkaline 5-c heme.

The 6-c hydroxide adducts present after the first two pH transitions exist in thermal spin-state equilibria, and the LS/HS ratio is independent of the total heme hydroxide concentration. These results reveal correlation between changes in heme and tyrosine spectroscopic signatures as a function of pH and the previously reported loss of kinase activity over the same pH range (*12*). Since the fraction of LS heme does not completely account for the loss of kinase activity between pH 8.5 and 11, a change in the H-bonding status of the tyrosine residue whose deprotonation tracks heme−OH formation may be responsible for the remaining loss of kinase activity due to diminished signal transmission. In this model, the aforementioned tyrosine would be critical to communication between the heme and kinase domains of FixL.

REFERENCES

1. He, Y., Shelver, D., Kerby, R. L., and Roberts, G. P. (1996) *J. Biol. Chem. 271*, 120−123.
2. Aono, S., Hakajima, H., Saito, K., and Okada, M. (1996) *Biochem. Biophys. Res. Commun. 228*, 752−756.
3. Garber, D. L., and Lowe, D. G. (1994) *J. Biol. Chem. 269*, 30741−30744.
4. Gilles-Gonzales, M. A., Gonzalez, G., Perutz, M. F., Kiger, L., Marden, M. C., and Poyrart, C. (1994) *Biochemistry 33*, 8067−8073.
5. David, M., Daveran, M. L., Batut, J., Dedieu, A., Domergue, O., Ghai, J., Hertig, C., Boistard, P., and Kahn, D. (1988) *Cell 54*, 671−683.
6. Gilles-Gonzalez, M. A., Ditta, G. S., and Helinski, D. R. (1991) *Nature 350*, 170−172.
7. Monson, E. K., Weinstein, M., Ditta, G. S., and Helinski, D. R. (1992) *Proc. Natl. Acad. Sci. U.S.A.* 89, 4280−4284.
8. Lois, A. F., Weinstein, M., Ditta, G. S., and Helinski, D. R. (1993) *J. Biol. Chem. 268*, 4370−4375.
9. Agron, P. G., Ditta, G. S., and Helinski, D. R. (1993) *Proc. Natl. Acad. Sci. U.S.A. 90*, 3506−3510.
10. Reyrat, J., David, M., Blonski, C., Boistard, P., and Batut, J. (1993) *J. Bacteriol. 175*, 6867−6872.
11. Galinier, A., Garnerone, A., Reyrat J., Kahn, D., Batut, J., and Boistard, P. (1994) *J. Biol. Chem. 269*, 23784−23789.
12. Gilles-Gonzalez, M. A., Gonzalez, G., and Perutz, M. F. (1995) *Biochemistry 34*, 232−236.
13. Winkler, W. C., Gonzalez, G., Wittenberg, J. B., Hille, R., Dakappagari, N., Jacob, A., Gonzalez, L. A., and Gilles-Gonzalez, M. A. (1996) *Chem. Biol. 3*, 841−850.
14. Beetlestone, J., and George, P. (1964) *Biochemistry 3*, 707−714.
15. George, P., Beetlestone, J., and Griffith, J. S. (1964) *Rev. Mod. Phys. 36*, 441−455.
16. Asher, S. A., Vickery, L. E., Schuster, T. M., and Sauer, K. (1977) *Biochemistry 16*, 5849−5856.
17. Asher, S. A., and Schuster, T. M. (1979) *Biochemistry 18*, 5377−5387.
18. Desbois, A., Lutz, M., and Banerjee, R. (1979) *Biochemistry 18*, 1510−1518.
19. Feis, A., Marzocchi, M. P., Paoli, M., and Smulevich, G. (1994) *Biochemistry 33*, 4577−4583.
20. Sitter, A. J., Shifflett, J. R., and Terner, J. (1988) *J. Biol. Chem. 263*, 13032−13038.
21. Takahashi, S., Wang, J., Rousseau, D. L., Ishikawa, K., Yoshida, T., Host, J. R., and Ikeda-Saito, M. (1994) *J. Biol. Chem. 269*, 1010−1014.
22. Takahashi, S., Wang, J., Rousseau, D. L., Ishikawa, K., Yoshida, T., Takeuchi, N., and Ikeda-Saito, M. (1994) *Biochemistry 33*, 5531−5538.
23. Ishikawa, K., Takeuchi, N., Takahashi, S., Matera, K. M., Sato, M., Shibahara, S., Rousseau, D. L., Ikeda-Saito, M., and Yoshida, T. (1995) *J. Biol. Chem. 270*, 6345−6350.
24. Smulevich, G., Neri, F., Marzocchi, M. P., and Welinder, K. G. (1996) *Biochemistry 35*, 10576−10585.
25. Smulevich, G., Miller, M. A., Kraut, J., and Spiro, T. G. (1991) *Biochemistry 30*, 9546−9558.
26. Howes, B. D., Rodriguez-Lopez, J. N., Smith, A. T., and Smulevich, G. (1997) *Biochemistry 36*, 1532−1543.
27. Rodgers, K. R., Lukat-Rodgers, G. S., and Barron, J. A. (1996) *Biochemistry 35*, 9539−9548.
28. Lukat-Rodgers, G. S., and Rodgers, K. R. (1997) *Biochemistry*, *36*, 4178−4187.
29. Antonini, E., and Brunori, M. *Frontier in Biology; Hemoglobin and Myoglobin in Their Reactions with Ligands* (1971) Vol. 21, North-Holland Publishing Co., Amsterdam.
30. Sun, J., Wilks, A., Ortiz de Montellano, P. R., and Loehr, T. M. (1993) *Biochemistry 32*, 14151−14157.
31. Monson, E. K., Ditta, G. S., and Helinski, D. R. (1995) *J. Biol. Chem. 270*, 5243−5250.
32. Rava, R. P., and Spiro, T. G. (1985) *J. Phys. Chem. 89*, 1856−1861.
33. Ludwig, M., and Asher, S. A. (1988) *J. Am. Chem. Soc. 110*, 1005−1011.
34. Makinen, M. W., and Churg, A. K. (1983) in *Iron Porphyrins Part One* (Lever, A. B. P., and Gray, H. B., Eds.) pp 141−236, Addison-Wesley, Reading, MA.
35. Drago, R. S. *Physical Methods for Chemists*, 2nd ed., pp 103−106, Surfside Scientific Publishers, Gainseville, FL.
36. Spiro, T. G., Stong, J. D., and Stein, P. (1979) *J. Am. Chem. Soc. 101*, 2648−2655.
37. Choi, S., Spiro, T. G., Langry, K. C., Smith, K. M., Budd, D. L., and LaMar, G. N. (1982) *J. Am. Chem. Soc. 104*, 4345−4351.
38. Lukat-Rodgers, G. S., and Rodgers, K. R. (1998) *JBIC, J. Biol. Inorg. Chem. 3*, 274−281.
39. Rousseau, D. L., Ching, Y., Brunori, M., and Giacometti, G. M. (1989) *J. Biol. Chem. 264*, 7878−7881.
40. Palaniappan. V., and Terner, J. (1989) *J. Biol. Chem. 264*, 16046−16053.
41. Smulevich, G., Mauro, J. M., Fishel, L. A., English, A. M., Kraut, J., and Spiro, T. G. (1988) *Biochemistry 27*, 5477−5485.
42. Spiro, T. G., and Li, X. Y. (1988) in *Biological Aplications of Raman Spectroscopy* (Spiro, T. G., Ed.) Vol. 3, pp 1−38, John Wiley & Sons, New York.
43. Palmer, G. (1985) *Biochem. Soc. Trans. 13*, 548−560.

44. Ikeda-Saito, M., Hori, H., Andersson, L. A., Prince, R. C., Pickering, I. J., George, G. N., Sanders, C. R., II, Lutz, R. S.,McKelvey, E. J., and Mattera, R. (1992) *J. Biol. Chem. 267*, 22843−22852.
45. Bogumil, R., Maurus, R., Hildebrand, D. P., Brayer, G. D., and Mauk, A. G. (1995) *Biochemistry 34*, 10483−10490.
46. Peisach, J., Blumberg, W. E., Ogawa, S., Rachmilewitz, E. A., and Oltzik, R. (1971) *J. Biol. Chem. 246*, 3342−3355.
47. Krauss, D. W., Wittenberg, J. B., Jing-Fen, L., and Peisach, J. (1990) *J. Biol. Chem. 265*, 16054−16059.
48. Rotilio, G., Calabrese, L., Giacometti, G. M., and Brunori, M. (1971) *Biochim. Biophys. Acta 236*, 234−237.
49. Appleby, C. A., Blumberg, W. E., Peisach, J., Wittenberg, B. A., and Wittenberg, J. B. (1976) *J. Biol. Chem. 251*, 6090−6096.
50. Tamura, K., Nakamura, H., Tanaka, Y., Oue, S., Tsukamoto, K., Normura, M., Tsuchiya, T., Adachi, S., Takahashi, Iizuka, T., and Shiro, Y. (1996) *J. Am. Chem. Soc. 118*, 9434- 9435..
51. Hu, S., Smith, K. M., and Spiro, T. G. (1996) *J. Am. Che. Soc. 118*, 12638−12646.
52. Smulevich, G., Hu, S., Rodgers, K. R., Goodin, D. B., Smith, K. M., and Spiro, T. G. (1996) *Biospectroscopy 2*, 365−376.
53. Hashimoto, S., Tatsuno, Y., and Kitagawa, T. (1986) *Proc. Natl. Acad. Sci. U.S.A. 83*, 2417−2422.
54. Hashimoto, S., Teraoka, J., Inubushi, T., Yonetani, T., and Kitagawa, T. (1986) *J. Biol. Chem. 261*, 11110−11117.
55. Teraoka, J., and Kitagawa, T. (1981) *J. Biol. Chem. 256*, 3969−3977.

BI981439V